Solar Phys (2014) 289:1531–1542
DOI 10.1007/s11207-013-0440-3

Temporal Evolution of Sunspot Areas and Estimation of Related Plasma Flows

R. Gafeira · C.C. Fonte · M.A. Pais · J. Fernandes

Received: 7 March 2013 / Accepted: 17 October 2013 / Published online: 16 November 2013

Abstract The increased amount of information provided by ongoing missions such as the *Solar Dynamics Observatory* (SDO) represents a great challenge for the understanding of basic questions such as the internal structure of sunspots and how they evolve with time. Here, we contribute with the exploitation of new data, to provide a better understanding of the separate growth and decay of sunspots, umbra, and penumbra. Using fuzzy sets to compute separately the areas of sunspot umbra and penumbra, the growth and decay rates for active regions NOAA 11117, NOAA 11428, NOAA 11429, and NOAA 11430 are computed from the analysis of intensitygrams obtained by the *Helioseismic and Magnetic Imager* onboard SDO. A simplified numerical model is proposed for the decay phase, whereby an empirical irrotational and uniformly convergent horizontal velocity field interacting with an axially symmetric and height-invariant magnetic field reproduces the large-scale features of the much more complex convection observed inside sunspots.

Keywords Sunspot area · Umbra · Penumbra · Fuzzy set · Fuzzy area

R. Gafeira (✉) · M.A. Pais · J. Fernandes
Center for Geophysics of the University of Coimbra, Coimbra, Portugal
e-mail: gafeira@mat.uc.pt

R. Gafeira · J. Fernandes
Astronomical Observatory of the University of Coimbra, Coimbra, Portugal

C.C. Fonte
Institute for Systems and Computers Engineering at Coimbra, Coimbra, Portugal

C.C. Fonte · J. Fernandes
Department of Mathematics, University of Coimbra, Coimbra, Portugal

M.A. Pais
Department of Physics, University of Coimbra, Coimbra, Portugal

1. Introduction

The emergence of the magnetic field through the photosphere has multiple manifestations, of which sunspots are the most prominent examples. Since the discovery of the solar cycle by Schwabe (1844), sunspots have been extensively studied from very different and complementary perspectives. For instance, we point out recent studies of the subphotosphere structure using magnetohydrodynamics (MHD) simulations (*e.g.* Cheung *et al.*, 2010) or the analysis of local helioseismology (*cf.* Kosovichev, 2012 and references therein). See also Moradi *et al.* (2010) for a general discussion on the subject. On the other hand, the sunspot number is a standard parameter used in long time-series analyses of the solar activity in the framework of space-weather studies (*e.g.* Messerotti *et al.*, 2009). During the past four decades, a great amount of data has been collected and several models have been proposed to explain the structure and evolution of sunspots (Solanki, 2003 and references therein). One of the most relevant sunspot properties for studying both its structure and evolution is the sunspot area, which can be the total area, or the umbral or penumbral area. The sunspot area has a considerable impact on solar activity, namely on the variation of the total radiance and the magnetic flux (Pettauer and Brandt, 1997). Moreover, both total and umbral areas are proxies of the sunspot magnetic-field strength (Jin *et al.*, 2006). Accordingly, one can find many articles dedicated to the study of the characteristics and evolution of sunspot areas. Some of the most important lines of research are the analysis of sunspot growth and decay (Chapman and Hoffer, 2006), the balance between the umbral and penumbral areas and its relation to the total sunspot brightness (Mathew *et al.*, 2007), and the stability of the total umbral area from one cycle to another, as supported by the analysis of long time-series covering several solar cycles (Bogdan *et al.*, 1988). Because of its relevance, large databases of sunspot areas have been built by different groups during the past years (*cf.* Zharkova *et al.*, 2005; Balmaceda *et al.*, 2009) to support the above studies. Simultaneously, a considerable effort has been applied on automatic detection of active regions (ARs) using different approaches and methods (*e.g.* Watson, Fletcher, and Marshall, 2011; Verbeeck *et al.*, 2011).

Modern solar instrumentation allows the analysis of sunspot evolution within time scales as short as one minute and even one second. As a result, the evolution of sunspots (areas) can be followed in detail. Schlichenmaier *et al.* (2010) studied the evolution of NOAA AR 11024 during a 4:40 time period, using data in the G-band and Ca II K from the German Vacuum Tower Telescope. They concluded that during the penumbral formation, the umbral area remains constant and the increase of the total sunspot area is caused exclusively by the penumbral growth. The penumbra region is located where the inclination of the magnetic field lines with respect to the direction of local gravity exceeds a critical value of about 30°. Schlichenmaier *et al.* (2010) observed that during sunspot growth penumbral filaments begin to form at the umbral boundary, but the umbral area is, basically, invariant with time. On this subject it is important to point out that recent observations of the three-minute oscillation over sunspot umbrae confirm a variation of the magnetic-field inclination inside the umbra, from 0° at the center to about 30° at the boundary (Reznikova *et al.*, 2012). Additionally, as pointed out by Javaraiah (2011),"the studies of growth and decay of sunspots or sunspot groups are important for understanding configuration and topology of the magnetic structure on the solar surface, the solar variability and the underlying mechanism of it."

It is reasonable to assume that sunspot evolution is intimately related to the plasma flow in the vicinity of the photosphere. Different techniques of tracking horizontal proper motions in the photosphere and subphotosphere have recently been developed, such as the feature-tracking (FT) and local-correlation tracking (LCT) methods for estimating surface plasma

velocities (*e.g.* Sobotka and Puschmann, 2009, Verma and Denker, 2011), and helioseismic techniques for assessing subphotospheric flows (*e.g.* Hindman, Haber, and Toomre, 2009; Zhao, Kosovichev, and Sekii, 2010). Liu, Zhao, and Schuck (2012) used the two methods to compare horizontal flow fields in the photosphere and subphotosphere. Understanding the observed features of sunspots as accurately as possible is a useful exercise for a more profound understanding of the solar surface/subsurface dynamics. Some recurring observational results concerning plasma flow and sunspots are i) conspicuous penumbral Evershed outflows of magnitude $1-4\ \mathrm{km\,s^{-1}}$, observed since 1909 and explained by recent numerical simulations (Kitiashvili *et al.*, 2009); ii) outgoing moat flows beyond the sunspot penumbra (*e.g.* Beauregard, Verma, and Denker, 2012; Liu, Zhao, and Schuck, 2012); and iii) inflows in the inner penumbra and umbra, detected with FT and LCT methods (*e.g.* Sobotka and Puschmann, 2009; Verma and Denker, 2011; Liu, Zhao, and Schuck, 2012; Beauregard, Verma, and Denker, 2012). The convective scenario in which these features coexist is still unclear. Moradi *et al.* (2010) proposed a schematic flow-structure of the large-scale circulations within active regions, with a mean inflow at the AR periphery and a stronger outflow closer to the surface at the core of the AR (sunspots). Liu, Zhao, and Schuck (2012), using FT and helioseismic methods, compared horizontal-flow fields in the photosphere and in a deeper layer 0.5 Mm below the photosphere in two solar AR. Their results picture a higher resolution flow structure inside the sunspot, with an inward flow inside the sunspot umbra and inner penumbra and an outward flow starting inside the penumbra and extending to the areas surrounding the sunspot. They found that the inward-flow area in the sunspot is larger at depth.

Since February 2010, the *Solar Dynamics Observatory* (SDO: Pesnell, Thompson, and Chamberlin, 2012) has been in orbit, monitoring the Sun and taking images with time scales and resolutions never achieved before. Fonte and Fernandes (2009) presented a new method for determining sunspot areas based on fuzzy sets. The method allows the penumbral area, umbral area, and their corresponding uncertainties to be determined automatically. This methodology is particularly suitable for use with high-resolution images such as those from the *Helioseismic and Magnetic Imager* (HMI: Schou *et al.*, 2012). Combining these observational and methodological developments, this article aims to analyze in detail the areal evolution of the ARs NOAA 11117, NOAA 11428, NOAA 11429, and NOAA 11430. A simplified MHD kinematic model to explain the areal evolution of the umbra/penumbra during the decay phase is also proposed.

This article is organized as follows: in Section 2 we describe the methodology to derive the umbral and penumbral areas based on a fuzzy-sets approach and present the results obtained for the evolution of the sunspot areas; in Section 3 we test a diffusion–advection numerical model based on the MHD equations to simulate the decay of one sunspot, and the last section is devoted to the discussion of results and conclusions.

2. ARs Area Computation

2.1. Data

The images treated in this study are intensitygrams obtained by the HMI installed onboard SDO. A set of images was analyzed for the following ARs: 583 images for NOAA AR 11117, obtained from 17:55 on 23 October 2010 to 19:55 on 29 October 2010; 733 images for NOAA AR 11428, from 00:15 on 4 March 2012 to 10:15 on 12 March 2012; 870 images for NOAA AR 11429, from 00:15 on 4 March 2012 to 23:45 on 13 March 2012; and 620

images for NOAA AR 11429, from 11:00 on 4 March 2012 to 16:15 on 11 March 2012. The images are in JPEG format and have a resolution of 4096 × 4096 pixels. In this work we used the images in JPEG instead of FITS format and confirmed that with the fuzzy method the difference in the areas obtained is only 5 %, which is smaller than the error due to other sources. Indeed, even a one-pixel uncertainty in sunspot radius will introduce an area error larger than 5 %, therefore this does not require the data to be reprocessed with FITS files.

With this option we have significantly reduced the amount of data stored and processed, which makes the process faster.

2.2. Fuzzy Areas of Sunspots

There is no well-defined criterion to separate the pixels that belong to the umbra from those belonging to the penumbra of sunspots, or between the pixels belonging to the penumbra and the photosphere, especially in high-resolution images. Differences in assigning pixels to the umbra, penumbra, or photosphere influence the results obtained for the area of these regions, and therefore these values are uncertain. One possible option to account for this uncertainty is to use approaches based on fuzzy sets, such as the one proposed by Fonte and Fernandes (2009) for HMI continuum images and by Barra *et al.* (2009) for solar extreme-ultraviolet (EUV) solar images. Here, we followed Fonte and Fernandes (2009) to compute the fuzzy umbra, fuzzy penumbra, and fuzzy sunspot area.

A fuzzy set A, defined in a universal set X, is characterized by a membership function $\mu_A(x)$ (Klir and Yuan, 1995), which expresses the degree of membership of each element of X to the fuzzy set. The degrees of membership typically take values between zero and one, where zero means no membership and one means full membership. In this application fuzzy sets corresponding to the umbra, penumbra, and sunspot are generated as a function of the radiation intensity registered in each pixel. To compute the degrees of membership to assign to the different intensity values, the proposed methodology uses a low-pass smoothing filter to decrease the variability of values of the pixels that belong to these three types of regions visible in high-resolution images. A histogram of the filtered image is then analyzed to determine the range of intensity values corresponding to the transition zones between the umbra and the penumbra, and between the penumbra and the photosphere. These values are used to generate membership functions of the intensity values to the umbra, penumbra, and photosphere, which are then used to compute the degrees of membership of each pixel to these regions, based on the pixel-intensity value. To determine the fuzzy areas of the fuzzy umbra, penumbra, and sunspot, the fuzzy-area operator described by Fonte and Fernandes (2009) and Fonte and Lodwick (2004) was used, which enables the identification of pixels for which the assignment to one of the regions (umbra, penumbra, or photosphere) is uncertain. The operator also evaluates the influence of these doubts in the area computation. This enables the quantification of uncertainty, and allows, among other things, the computation of maximum and minimum area values for the umbra, penumbra, and photosphere, which correspond to the area obtained considering the pixels with degrees of membership to each region larger than zero and equal to one, respectively.

2.3. Results of the Group Area Analysis

The methodology was applied to the data described in Section 2.1. In the filtering process, a five-by-five-pixel window was used, considering equal weights for all pixels. The filter ran three times for each image. Figures 1, 2, 3, and 4 show the area values (in millionths of the area of a visible solar hemisphere: μHem) of the ARs analyzed during the sunspot growth and decay as a function of time.

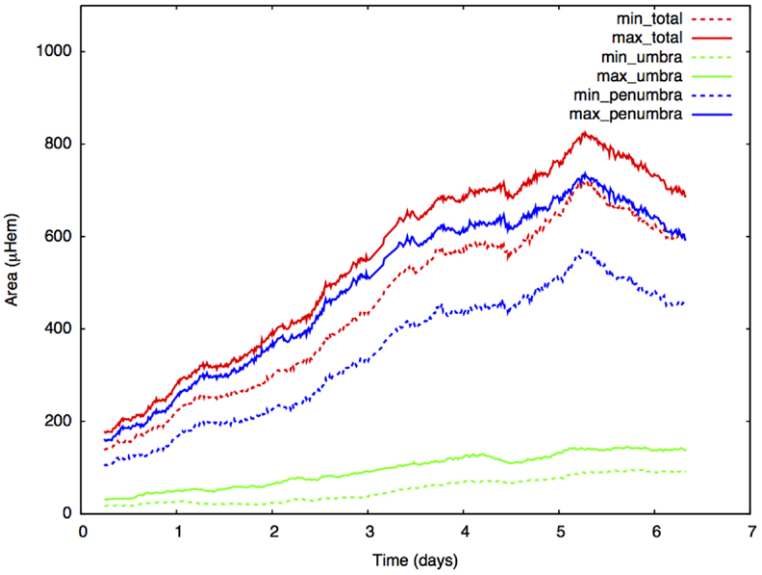

Figure 1 Area evolution of NOAA AR 11117: lowest (dashed lines) and highest (solid lines) fuzzy-area estimates for the total sunspot area (red lines), the umbra (green lines), and the penumbra (blue lines).

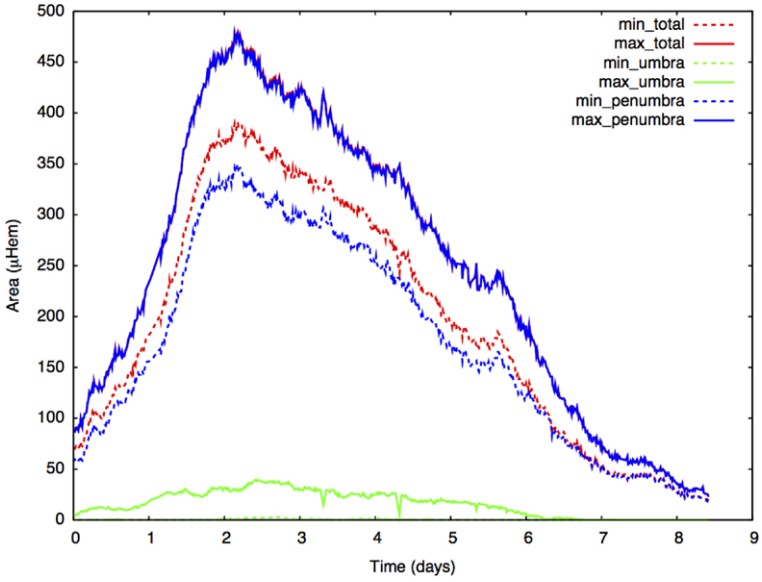

Figure 2 Area evolution of NOAA AR 11428: lowest (dashed lines) and highest (solid lines) fuzzy-area estimates for the total sunspot area (red lines), the umbra (green lines), and the penumbra (blue lines).

Area growth and decay rates ($\mathrm{d}A/\mathrm{d}t$) were computed for each sunspot feature (umbra, penumbra, and total sunspot) by fitting a linear regression model to the area evolution curves shown in Figures 1 to 4. Using the maximum and minimum values obtained for the fuzzy

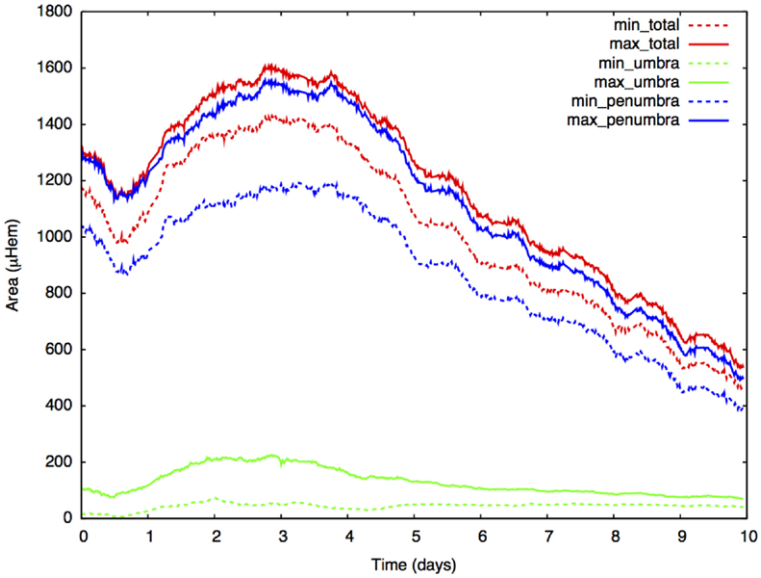

Figure 3 Area evolution of NOAA AR 11429: lowest (dashed lines) and highest (solid lines) fuzzy-area estimates for the total sunspot area (red lines), the umbra (green lines), and the penumbra (blue lines).

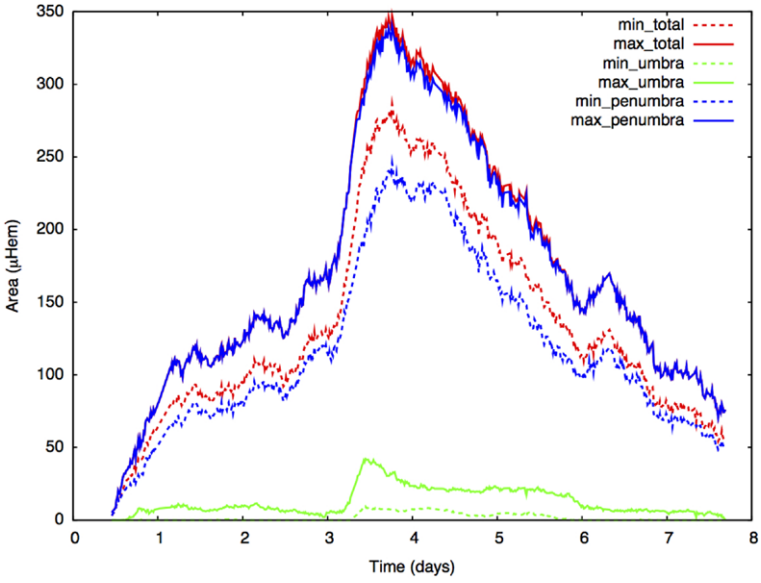

Figure 4 Areal evolution of NOAA AR 11430: lowest (dashed lines) and highest (solid lines) fuzzy-area estimates for the total sunspot area (red lines), the umbra (green lines), and the penumbra (blue lines).

area of the umbra, penumbra, and total sunspot (shown in Figure 1), two different estimates were obtained for the increase or decrease rate of these regions. The difference between the two values provides an estimate of the uncertainty associated to the increase/decrease

Table 1 Growth phase of AR feature areas.

NOAA AR	Min/max values total area [μHem]	Min/max rate values global sunspot [μHem day^{-1}]	Min/max rate values penumbra [μHem day^{-1}]	Min/max rate values umbra [μHem day^{-1}]
11117	720/820	113/130	90/115	14/22
11428	390/480	165/201	148/201	0/12
11429	1420/1600	181/196	123/180	16/56
11430	295/350	267/300	199/283	16/68

Table 2 Decay phase of AR feature areas.

NOAA AR	Min/max values total area [μHem]	Min/max rate values global sunspot [μHem day^{-1}]	Min/max rate values penumbra [μHem day^{-1}]	Min/max rate values umbra [μHem day^{-1}]
11117	720/820	−116/−126	−112/−127	1/−1
11428	390/480	−77/−85	−66/−85	0/−8
11429	1420/1600	−121/−142	−108/−141	−1/−10
11430	295/350	−71/−84	−65/−81	−3/−4

rate. The results are shown in Tables 1 and 2. The values obtained are on the same order of magnitude as those presented by Hathaway and Choudhary (2008), who found a decay rate of $\mathrm{d}A/\mathrm{d}t = -150\,\mu\mathrm{Hem\,day}^{-1}$ for AR 9415 one day after the largest area value was attained. They also confirmed the observations of Schlichenmaier *et al.* (2010), which indicate that the growth and decay of the penumbra is the largest contributor to the total-area evolution and that umbral growth and decay rates are much lower.

3. Simulation of Sunspot Area Decay

We focused our analysis on the sunspot decay phase which, as pointed out by different authors (*e.g.* Bellot Rubio, Tritschler, and Martínez Pillet, 2008), is less well understood than penumbral formation and growth. It is assumed that the main features of the umbral and penumbral decay phases can be captured with the approximation of cylindrical symmetry relative to the sunspot axis and a negligible height dependence. Denoting cylindrical coordinates by (r, θ, z), where r is the distance to the axis, θ is the azimuthal angle, and z is the height above the photosphere, all partial derivatives with respect to z and θ are zero. The first step was to investigate whether the sunspot behavior during the decay phase could be an effect of diffusion, either ohmic or turbulent. The system of equations describing diffusion of a poloidal magnetic field with the assumed symmetry is given by

$$\frac{\partial B_z}{\partial t} = \eta \nabla^2 B_z, \tag{1}$$

$$\frac{\partial B_\mathrm{r}}{\partial t} = \eta \left(\nabla^2 B_\mathrm{r} - \frac{B_\mathrm{r}}{r^2} \right), \tag{2}$$

where $B_z(r,t)$ and $B_r(r,t)$ are the axial and radial magnetic-field components, t is the time, and η is the magnetic diffusivity. The ∇^2 operator is given by

$$\nabla^2 = \frac{1}{r}\frac{\partial}{\partial r}\left(r\frac{\partial}{\partial r}\right).$$

The differential equations (1) and (2) can be analytically solved using separation of variables. As boundary conditions, we require that both B_z and B_r must be finite at the sunspot axis ($r = 0$). The outer boundary conditions as well as the initial conditions [$B_z(r/r_0, 0)$ and $B_r(r/r_0, 0)$] are obtained from Borrero and Ichimoto (2011), who computed the radial variation of azimuthally averaged vertical and horizontal components of the magnetic field from the inversion of spectropolarimetric observations employing a Milne–Eddington atmospheric model. We found for the two initial radial functions [$B_z(r/r_0, 0)$ and $B_r(r/r_0, 0)$] a combination of Bessel functions of the first kind of about 0 and 1, respectively. These initial functions, which very closely represent the Borrero and Ichimoto (2011) model for AR 10933 (see Figure 11 in Borrero and Ichimoto, 2011) as shown in Figure 5, are expressed by Equations (3) and (4),

$$\begin{aligned} B_z(r/r_0) &= 1166.51 J_0(k_{1,0} r/r_0) + 1157.55 J_0(k_{2,0} r/r_0) \\ &\quad + 382.855 J_0(k_{3,0} r/r_0) + 162.414 J_0(k_{4,0} r/r_0), \end{aligned} \tag{3}$$

$$\begin{aligned} B_r(r/r_0) &= 1688.57 J_1(k_{1,1} r/r_0) + 530.185 J_1(k_{2,1} r/r_0) \\ &\quad + 428.751 J_1(k_{3,1} r/r_0), \end{aligned} \tag{4}$$

where $r_0 = 1.5 R_S$ with R_S the initial sunspot radius, $k_{m,0}$ is the m-th root of $J_0(r/r_0)$, and $k_{m,1}$ is the m-th root of $J_1(r/r_0)$. According to Borrero and Ichimoto (2011), the umbra/penumbra and the penumbra/moat separation conditions are $B_r/B_z = \tan 35^\circ$ and $B_r/B_z = \tan 77^\circ$, respectively. Based on Figure 11 in Borrero and Ichimoto (2011), we used variance values of $\sigma^2_{B_z} = 100^2 G^2$ and $\sigma^2_{B_r} = 200^2 G^2$ for the fit of our Equations (3) and (4) to the Borrero and Ichimoto (2011) radial model. We obtained χ^2 values $\chi^2_{B_z} = 0.006$ and $\chi^2_{B_r} = 0.07$, respectively, for the two fits. Our initial solution is also very close to the buried-dipole solution (Solanki, 2003) for a dipole magnetic moment of 1.25×10^{23} Am^2 and a dipole depth of 20 470 km.

Accordingly, the diffusion process can be described in terms of the exponential decay of just a few modes, each one evolving with a characteristic time scale,

$$B_z(r/r_0, t) = \sum_{m=1}^{4} A_m J_0(k_{m,0} r/r_0) \exp\left(-\eta k^2_{m,0} t/r_0^2\right), \tag{5}$$

$$B_r(r/r_0, t) = \sum_{m=1}^{3} A_m J_1(k_{m,1} r/r_0) \exp\left(-\eta k^2_{m,1} t/r_0^2\right). \tag{6}$$

The important point to realize here is that the temporal evolution of the sunspot geometry during a purely diffusive process is entirely determined by the relative contribution of different modes for $B_z(r/r_0)$ and $B_r(r/r_0)$. In particular, because the most important mode in $B_z(r/r_0)$ decays with a time scale of $r_0^2/(k^2_{1,0}\eta)$, where $k^2_{1,0} = 5.78$, longer than the dominant time scale $[r_0^2/(k^2_{1,1}\eta)]$ of B_r decay, where $k^2_{1,1} = 14.68$, the inclination of the magnetic-field lines at a certain point inside the sunspot decreases with time, and as a result the umbral area increases with time. This result, which is independent of the value adopted for the magnetic diffusivity as long as it is the same for both Equations (1) and (2), is incompatible with observations.

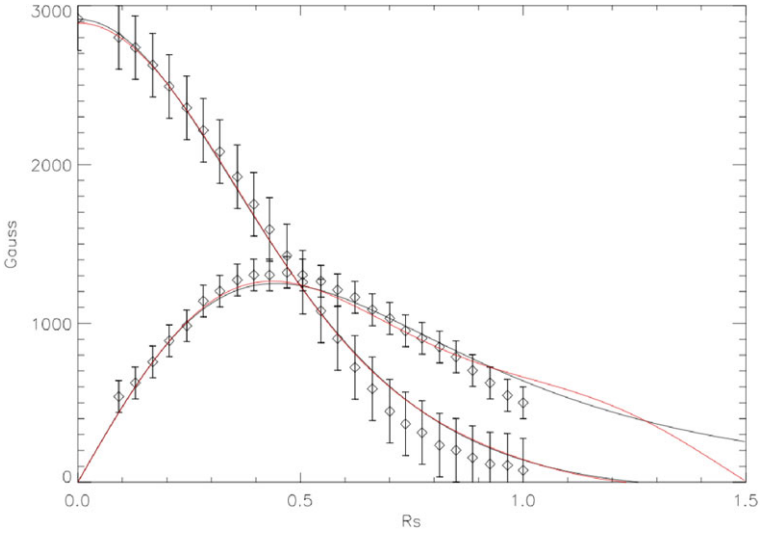

Figure 5 For the sunspot magnetic-field components B_z and B_r of AR 10933: radial model (Borrero and Ichimoto, 2011, white diamonds) with error bars, best buried-dipole model (Solanki, 2003, black lines), and the model proposed in this article of free decay cylindrical modes (red lines).

Inward advection of the magnetic-field lines by the plasma flow can counteract the effect of diffusion for adequately chosen velocity values. To simulate this effect, a simplified kinematic model was tested, for which the advection and stretching of the magnetic field by the photospheric plasma is the main mechanism responsible for the sunspot global area decay. In the approximation of a radial sunspot, the plasma velocity field is of the form $\mathbf{u} = u_r(r)\hat{\mathbf{r}}$ and the induction equations to solve are (7) and (8):

$$\frac{\partial B_z}{\partial t} = -u_r \frac{\partial B_z}{\partial r} + \eta \nabla^2 B_z, \tag{7}$$

$$\frac{\partial B_r}{\partial t} = B_r \frac{\partial u_r}{\partial r} - u_r \frac{\partial B_r}{\partial r} + \eta \left(\nabla^2 B_r - \frac{B_r}{r^2} \right). \tag{8}$$

Furthermore, because the observed decrease of the penumbral area is steeper than the observed umbral-area decrease, we can anticipate that the penumbra is affected by a higher inward flow than the umbra. The velocity field made to interact with the magnetic field is radial and of the form $u_r = u_0 r / R_S$, where r is the radial coordinate and R_S is the initial sunspot radius. To simulate the diffusion effect, an ohmic diffusivity of $\eta = 0.2\ \mathrm{km^2\ s^{-1}}$ was used, as estimated by Chae, Litvinenko, and Sakurai (2008).

For each of the four ARs NOAA 11117, 11428, 11429, and 11430, the u_0-parameter was adjusted such that the linear fit to the simulated sunspot decay very closely reproduced the linear fit to the observed sunspot decay (see Table 2). The result for AR 11117 is shown in Figure 6. Table 3 shows the numerical values found for u_0, together with initial sunspot areas $[A_S]$ and initial sunspot radius $[R_S]$ of different ARs. The two estimates shown for each one of the parameters u_0, A_S, and R_S correspond to fits made to the smallest and largest fuzzy-area curves shown in Figures 1 to 4. We considered as estimates for the error of u_0 $[\sigma_{u_0}]$ the differences between the estimated u_0-values using the smallest and largest fuzzy areas.

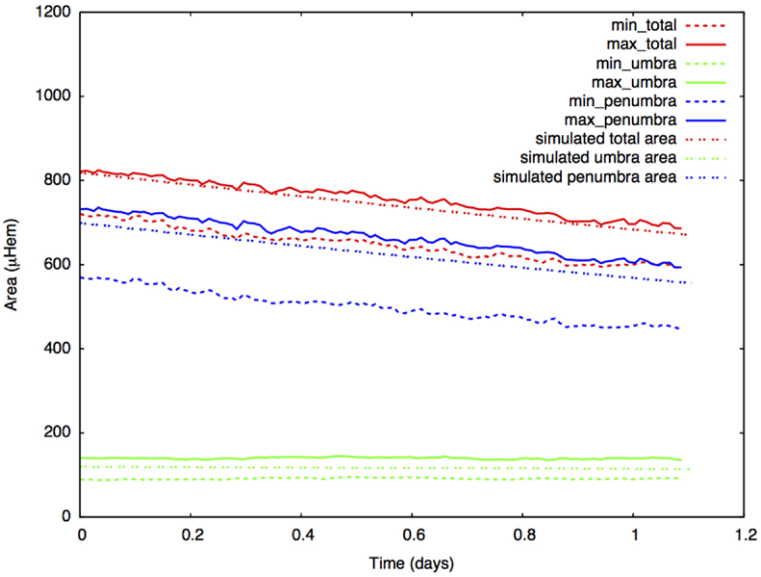

Figure 6 Decay phase of areal evolution for NOAA AR 11117 and corresponding simulated curves. Simulated values (intermittent dashed lines), lowest fuzzy estimates (dashed lines) and highest fuzzy estimates (solid lines) for the total sunspot area (red lines), the umbra (green lines), and the penumbra (blue lines).

Table 3 Fitted values of u_0 (lowest/highest) for the four case studies considered. Also shown are the times used for estimating the linear decay rate [Δt], the initial (smallest/largest) sunspot area [A_S], the initial (smallest/largest) sunspot radius [R_S], and the error estimate associated with the choice of u_0 [σ_{u_0}].

AR NOAA	Δt [days]	A_S [μHem]	R_S [Mm]	u_0 [$m\,s^{-1}$]	σ_{u_0} [$m\,s^{-1}$]
11117	1.5	720/820	26.41/27.84	−34.6/−35.3	0.7
11428	4.0	390/480	19.44/21.57	−59.0/−48.0	11.0
11429	6.0	1420/1600	37.09/39.37	−32.0/−35.0	3.0
11430	2.5	295/350	16.01/18.42	−44.0/−48.0	4.0

4. Discussion and Conclusions

Recently, Schlichenmaier *et al.* (2010) studied the evolution of NOAA AR 11024, concluding that during the penumbral formation the umbral area remains constant and that the increase of the total sunspot area is caused exclusively by the penumbral growth.

The results obtained in this study for the area evolution using the fuzzy-area estimation support the conclusions of Schlichenmaier *et al.* (2010). In fact, taking into account the short temporal duration of the observations in their study (only 4.7 hours), it is possible that the umbral growth could not be perceived if, as we see here, its growth rate was much lower than that of the penumbra.

A numerical kinematic model was tested in which the advection and stretching of the magnetic field by the photospheric plasma is the main mechanism responsible for the sunspot area decay. A z-independent initial solution for the sunspot's magnetic field was used, in agreement with the underlying assumptions. The obtained results support previous

claims that the advection of the field due to an inflow inside an AR with speeds between 10 and 100 m s^{-1} should be required to balance the outward transport of magnetic field by turbulent diffusion (Hurlburt and DeRosa, 2008). According to Hurlburt and DeRosa's numerical simulations of compressible magnetoconvection with flux-dependent surface cooling, the inflow inside ARs is driven by buoyancy as a result of localized surface cooling inside ARs. Our estimates for the highest speed [u_0] that occurs at the penumbra periphery, with values lying between 32 – 59 m s^{-1} for the case studies considered, does in fact match the order of magnitude of the Hurlburt and DeRosa (2008) large-scale inflows. Our results are compatible with the well-known Evershed outflows, since as shown by Kitiashvili *et al.* (2009), low-magnitude inflows of umbral and penumbral features can coexist with Evershed outflows as part of overturning convection motions. We expect that thanks to the high-quality instrumentation onboard of SDO or *Hinode* and with the existing tools from helioseismology and photospheric feature-tracking it will be possible in the future to test the numerical predictions presented in this article for a large number of ARs.

Acknowledgements The authors wish to thank NASA/SDO and the HMI science team for providing the HMI images and the referee for constructive comments that helped to improve the manuscript. MAP is supported by FCT (PTDC/CTE-GIX/119967/2010) through the project COMPETE (FCOMP-01-0124-FEDER-019978). CFC's work was partially supported by Fundação para a Ciência e a Tecnologia (FCT) under project grant PEst-C/EEI/UI0308/2011.

References

Balmaceda, L.A., Solanki, S.K., Krivova, N.A., Foster, S.: 2009, A homogeneous database of sunspot areas covering more than 130 years. *J. Geophys. Res.* **114**, 7104. doi:10.1029/2009JA014299.

Barra, V., Delouille, V., Kretzschmar, M., Hochedez, J.-F.: 2009, Fast and robust segmentation of solar EUV images: algorithm and results for solar cycle 23. *Astron. Astrophys.* **505**, 361 – 371. doi:10.1051/0004-6361/200811416.

Beauregard, L., Verma, M., Denker, C.: 2012, Horizontal flows concurrent with an X2.2 flare in the active region NOAA 11158. *Astron. Nachr.* **333**, 125. doi:10.1002/asna.201111631.

Bellot Rubio, L.R., Tritschler, A., Martínez Pillet, V.: 2008, Spectropolarimetry of a decaying sunspot penumbra. *Astrophys. J.* **679**, 676 – 698. doi:10.1086/527366.

Bogdan, T.J., Gilman, P.A., Lerche, I., Howard, R.: 1988, Distribution of sunspot umbral areas – 1917 – 1982. *Astrophys. J.* **327**, 451 – 456. doi:10.1086/166206.

Borrero, J.M., Ichimoto, K.: 2011, Magnetic structure of sunspots. *Liv. Rev. Solar Phys.* **8**, 4. doi:10.12942/lrsp-2011-4.

Chae, J., Litvinenko, Y.E., Sakurai, T.: 2008, Determination of magnetic diffusivity from high-resolution solar magnetograms. *Astrophys. J.* **683**, 1153 – 1159. doi:10.1086/590074.

Chapman, G.A., Hoffer, A.S.: 2006, The growth of facular area surrounding large, decaying sunspots. *Solar Phys.* **237**, 321 – 328. doi:10.1007/s11207-006-0118-1.

Cheung, M.C.M., Rempel, M., Title, A.M., Schüssler, M.: 2010, Simulation of the formation of a solar active region. *Astrophys. Space Sci.* **720**, 233 – 244. doi:10.1088/0004-637X/720/1/233.

Fonte, C.C., Fernandes, J.: 2009, Application of fuzzy sets to the determination of sunspot areas. *Solar Phys.* **260**, 21 – 41. doi:10.1007/s11207-009-9436-4.

Fonte, C.C., Lodwick, W.A.: 2004, Areas of fuzzy geographical entities. *Int. J. Geogr. Inf. Sci.* **18**(2), 127 – 150.

Hathaway, D.H., Choudhary, D.P.: 2008, Sunspot group decay. *Solar Phys.* **250**, 269 – 278. doi:10.1007/s11207-008-9226-4.

Hindman, B.W., Haber, D.A., Toomre, J.: 2009, Subsurface circulations within active regions. *Astrophys. J.* **698**, 1749 – 1760. doi:10.1088/0004-637X/698/2/1749.

Hurlburt, N., DeRosa, M.: 2008, On the stability of active regions and sunspots. *Astrophys. J. Lett.* **684**(2), L123. doi:10.1086/591736.

Javaraiah, J.: 2011, Long-term variations in the growth and decay rates of sunspot groups. *Solar Phys.* **270**, 463 – 483. doi:10.1007/s11207-011-9768-8.

Jin, C.L., Qu, Z.Q., Xu, C.L., Zhang, X.Y., Sun, M.G.: 2006, The relationships of sunspot magnetic field strength with sunspot area, umbral area and penumbra-umbra radius ratio. *Astrophys. Space Sci.* **306**, 23 – 27. doi:10.1007/s10509-006-9217-6.

Kitiashvili, I.N., Kosovichev, A.G., Wray, A.A., Mansour, N.N.: 2009, Traveling waves of magnetoconvection and the origin of the evershed effect in sunspots. *Astrophys. J. Lett.* **700**, L178 – L181. doi:10.1088/0004-637X/700/2/L178.

Klir, G.J., Yuan, B.: 1995, *Fuzzy Sets and Fuzzy Logic: Theory and Applications*, 1st edn., Prentice Hall PTR, Englewood Cliffs. ISBN 0131011715.

Kosovichev, A.G.: 2012, Local helioseismology of sunspots: current status and perspectives. *Solar Phys.* **279**, 323 – 348. doi:10.1007/s11207-012-9996-6.

Liu, Y., Zhao, J., Schuck, P.W.: 2012, Horizontal flows in the photosphere and subphotosphere of two active regions. *Solar Phys.* **287**, 279 – 291. doi:10.1007/s11207-012-0089-3.

Mathew, S.K., Martínez Pillet, V., Solanki, S.K., Krivova, N.A.: 2007, Properties of sunspots in cycle 23. I. Dependence of brightness on sunspot size and cycle phase. *Astron. Astrophys.* **465**, 291 – 304. doi:10.1051/0004-6361:20066356.

Messerotti, M., Zuccarello, F., Guglielmino, S.L., Bothmer, V., Lilensten, J., Noci, G., Storini, M., Lundstedt, H.: 2009, Solar weather event modelling and prediction. *Space Sci. Rev.* **147**, 121 – 185. doi:10.1007/s11214-009-9574-x.

Moradi, H., Baldner, C., Birch, A.C., Braun, D.C., Cameron, R.H., Duvall, T.L., Gizon, L., Haber, D., Hanasoge, S.M., Hindman, B.W., Jackiewicz, J., Khomenko, E., Komm, R., Rajaguru, P., Rempel, M., Roth, M., Schlichenmaier, R., Schunker, H., Spruit, H.C., Strassmeier, K.G., Thompson, M.J., Zharkov, S.: 2010, Modeling the subsurface structure of sunspots. *Solar Phys.* **267**, 1 – 62. doi:10.1007/s11207-010-9630-4.

Pesnell, W.D., Thompson, B.J., Chamberlin, P.C.: 2012, The Solar Dynamics Observatory (SDO). *Solar Phys.* **275**, 3 – 15. doi:10.1007/s11207-011-9841-3.

Pettauer, T., Brandt, P.N.: 1997, On novel methods to determine areas of sunspots from photoheliograms. *Solar Phys.* **175**, 197 – 203. doi:10.1023/A:1004903201224.

Reznikova, V.E., Shibasaki, K., Sych, R.A., Nakariakov, V.M.: 2012, Three-minute oscillations above sunspot umbra observed with the Solar Dynamics Observatory/Atmospheric Imaging Assembly and Nobeyama radioheliograph. *Astrophys. J.* **746**, 119. doi:10.1088/0004-637X/746/2/119.

Schlichenmaier, R., Bello González, N., Rezaei, R., Waldmann, T.A.: 2010, The role of emerging bipoles in the formation of a sunspot penumbra. *Astron. Nachr.* **331**, 563. doi:10.1002/asna.201011372.

Schou, J., Scherrer, P.H., Bush, R.I., Wachter, R., Couvidat, S., Rabello-Soares, M.C., Bogart, R.S., Hoeksema, J.T., Liu, Y., Duvall, T.L., Akin, D.J., Allard, B.A., Miles, J.W., Rairden, R., Shine, R.A., Tarbell, T.D., Title, A.M., Wolfson, C.J., Elmore, D.F., Norton, A.A., Tomczyk, S.: 2012, Design and ground calibration of the Helioseismic and Magnetic Imager (HMI) instrument on the Solar Dynamics Observatory (SDO). *Solar Phys.* **275**, 229 – 259. doi:10.1007/s11207-011-9842-2.

Schwabe, M.: 1844, Sonnenbeobachtungen im Jahre 1843. Von Herrn Hofrath Schwabe in Dessau. *Astron. Nachr.* **21**, 233.

Sobotka, M., Puschmann, K.G.: 2009, Morphology and evolution of umbral dots and their substructures. *Astron. Astrophys.* **504**, 575 – 581. doi:10.1051/0004-6361/200912365.

Solanki, S.K.: 2003, Sunspots: an overview. *Astron. Astrophys. Rev.* **11**, 153 – 286. doi:10.1007/s00159-003-0018-4.

Verbeeck, C., Higgins, P.A., Colak, T., Watson, F.T., Delouille, V., Mampaey, B., Qahwaji, R.: 2011, A multi-wavelength analysis of active regions and sunspots by comparison of automatic detection algorithms. *Solar Phys.* **283**, 67 – 95. doi:10.1007/s11207-011-9859-6.

Verma, M., Denker, C.: 2011, Horizontal flow fields observed in *Hinode* G-band images. I. Methods. *Astron. Astrophys.* **529**, A153. doi:10.1051/0004-6361/201016358.

Watson, F.T., Fletcher, L., Marshall, S.: 2011, Evolution of sunspot properties during solar cycle 23. *Astron. Astrophys.* **533**, A14. doi:10.1051/0004-6361/201116655.

Zhao, J., Kosovichev, A.G., Sekii, T.: 2010, High-resolution helioseismic imaging of subsurface structures and flows of a solar active region observed by *Hinode*. *Astrophys. J.* **708**, 304 – 313. doi:10.1088/0004-637X/708/1/304.

Zharkova, V.V., Aboudarham, J., Zharkov, S., Ipson, S.S., Benkhalil, A.K., Fuller, N.: 2005, Solar feature catalogues in Egso. *Solar Phys.* **228**, 361 – 375. doi:10.1007/s11207-005-5623-0.